# Optomechanical Design of Nine Cameras for the Earth Observing Systems Multi-Angle Imaging Spectral Radiometer, TERRA Platform

Virginia G. Ford, Mary L. White, Eric Hochberg, and Jim McGown
Jet Propulsion Laboratory
California Institute of Technology

## ABSTRACT

The Multi-Angle Imaging Spectral Radiometer (MISR) is a push-broom instrument using nine cameras to collect data at nine different angles through the atmosphere. The science goals are to monitor global atmospheric particulates, cloud movements, and vegetative changes. The camera optomechanical requirements were: to operate within specification over a temperature range of 0C to 10C; to survive a temperature range of –40C to 80C; to survive launch loads and on-orbit radiation; to be non-contaminating both to itself and to other instruments; and to remained aligned though the mission. Each camera has its own lens, detector, and thermal control. The lenses are refractive; thus passive thermal focus compensation and maintaining lens positioning and centering were dominant issues. Because of the number of cameras, modularity was stressed in the design.

This paper will describe the final design of the cameras, the driving design considerations, and the results of qualification testing.

Keywords: Optomechanical, refractive lens, passive thermal compensation, lens positioning, MISR, lens centering
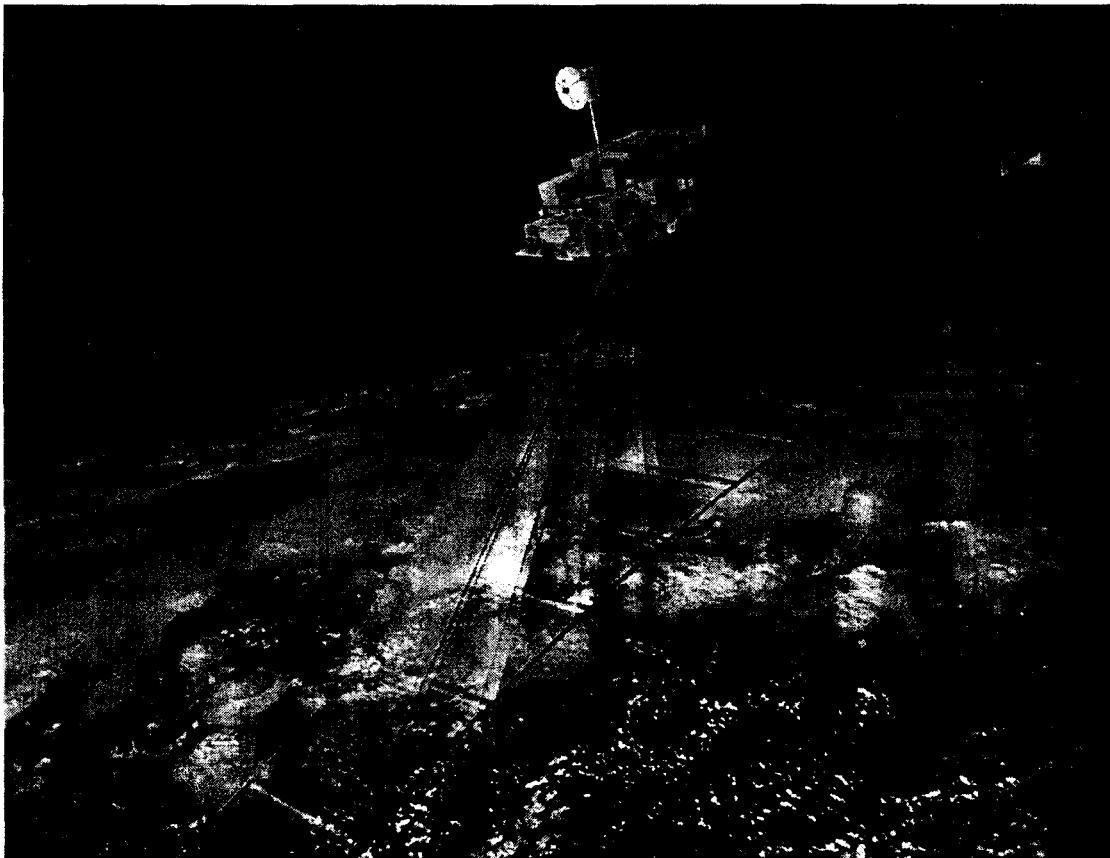
Figure 1. EOS-TERRA spacecraft with the Multi-Angle Imaging Spectral Radiometer instrument. The nine camera fields- of-view with four spectral wavebands are shown.
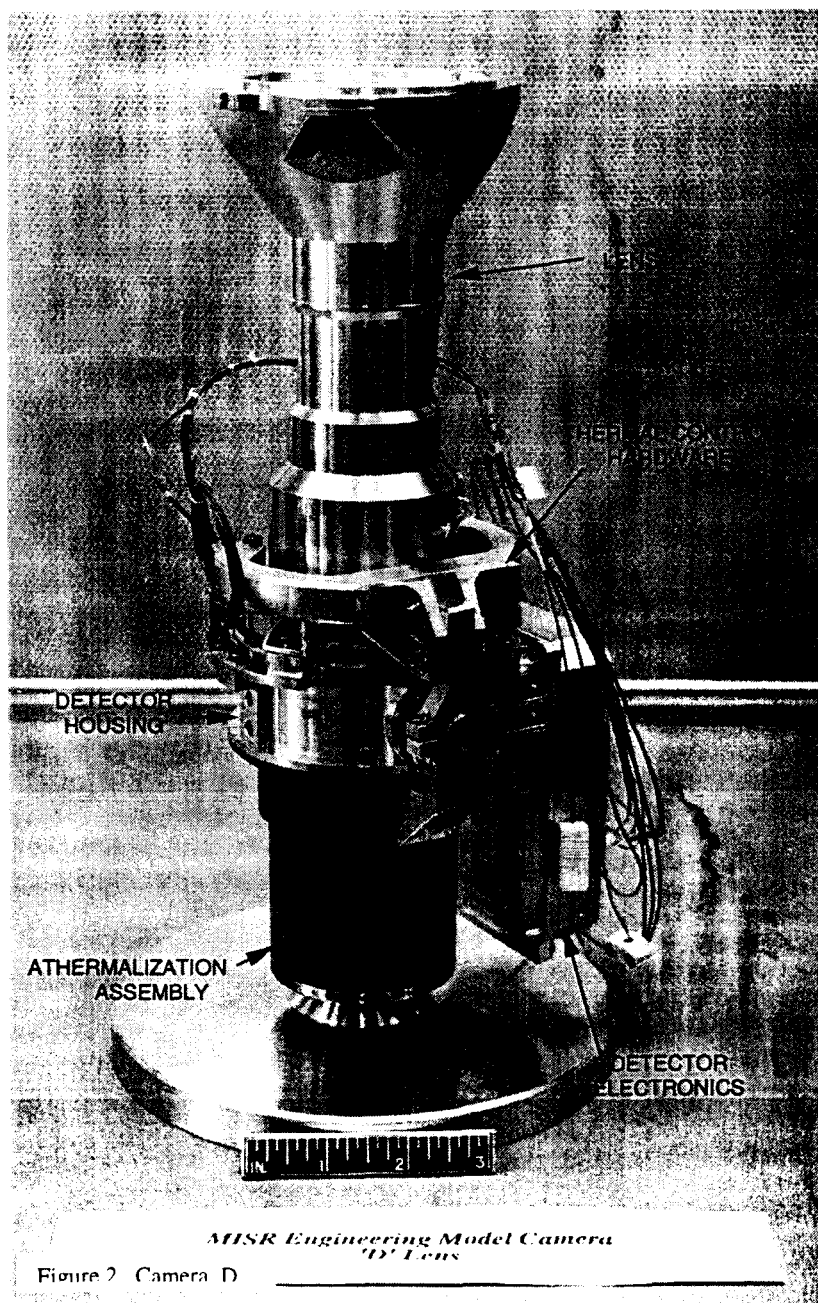
# 1. INTRODUCTION

MISR is mounted on the EOS-TERRA spacecraft, which will orbit around the Earth for up to a six-year mission. The spacecraft will be launched on an ATLAS IIAS rocket from Vanderberg Airforce Base – the launch is currently scheduled on August 27, 1999. All the instruments on the EOS-TERRA spacecraft monitor changes on the Earth that may affect its climatic balance.

The MISR instrument collects data that can be used to measure changes in top-of-atmosphere readings, clouds and surface angular reflectance functions. The instrument cameras also view through the atmosphere to measure surface BRDF, aerosol and vegetation properties. By measuring how much sunlight is scattered in different directions under natural conditions, the data collected by MISR will help to quantify the amount of solar energy heating the Earth's surface and atmosphere and the changes in these quantities that occur over the six-year nominal lifetime of the instrument. A push-broom instrument has stationary detectors that pass over the imaged scene while the spacecraft moves around the Earth. The data collected by the first camera of a position on the ground is tagged then compared to the data collected by the second, third and subsequent cameras. Examination of the data from the nine cameras for each place on the ground allows comparison of the differences and similarities caused by the different angle views. For further explanation of the scientific uses planned for data from this instrument, the Internet site, http://www-misr.jpl.nasa.gov/misci.html can be visited.



*MISR Engineering Model Camera*
*'D' Lens*

Figure 2. Camera D

# 2. CAMERA DESIGN CHOICES

In the MISR instrument, each camera looks continuously through an angle of atmosphere and focuses at the surface of the Earth. The cameras have matching footprint widths on the ground – except for the nadir footprint which is smaller than the others. The detector of each camera is a CCD that is preceded by spectral filters to receive four spectral bands within the range of 440 nanometers (nm) through 880 nm. The radiation environment encountered while the spacecraft passes over the poles was handled by using thick lens barrels (about 0.250 inches wall thickness). The selected glass types were tested for radiation darkening with both protons and electrons. The predicted loss of transmittance over the mission was within the specification. The thermal range expected is large enough to cause design challenges that will be discussed. The severity of launch loads influenced the lens mounting technique. Cleanliness and low outgassing characteristics were achieved through material choices and rigorous cleaning and bake-out procedures.

Each camera consists of a lens, a detector, passive athermalization assembly and thermal control hardware. Modularity was used where possible – with modular detectors, filters, passive athermalization design, and thermal control. In addition, the lens designs were all similar and had similar de-polarization hardware.
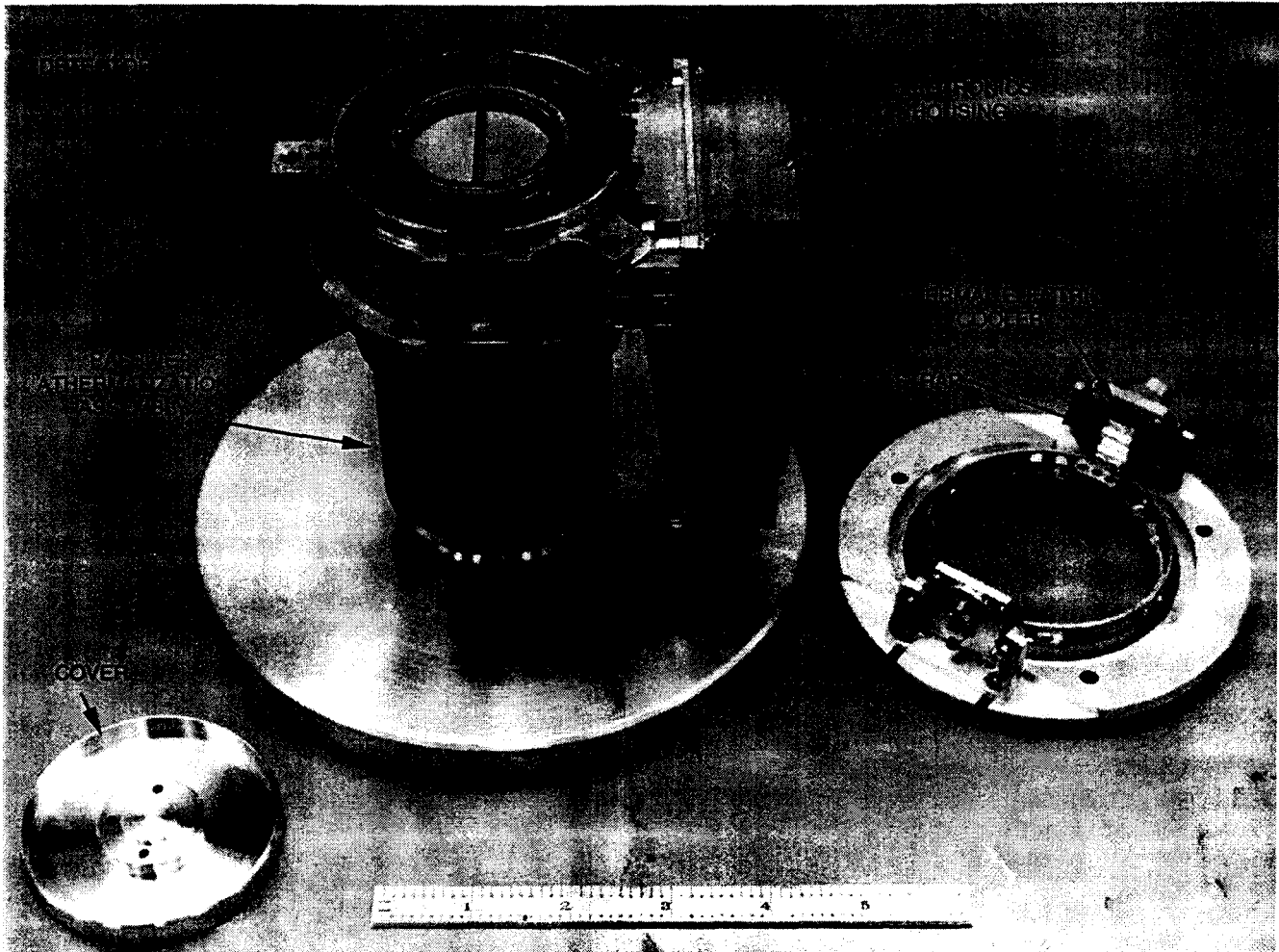


Figure 3. MISR modular camera head consisting of detector housing, electronics, and passive athermalization assembly

To reduce costs, four lens designs were chosen for the nine cameras shown in Figure 2. Angles were chosen so that each lens could be used both looking forward and rearward, with a nadir looking lens identical to the middle two lenses. The lenses used are designated A, B, C, and D with A being the shortest focal length and D being the longest. Lens A is the design used for the nadir-looking camera. The nine cameras are designated by the lens type and the direction - F for forward, A for aft, and N for nadir, thus they are called: DF, CF, BF, AF, AN, AA, BA, CA, and DA.

To develop small cameras, refractive lenses were chosen. Maintaining lens element positioning, centering, and clamping through the thermal environment and through the launch vibration environment were dominant issues in the design. Also, because the index of refraction of the glasses changes with temperature, passive thermal focus compensation had to be incorporated in each camera. In order for the passive athermalization to work well, it was important that the camera housing and lens barrel have small thermal gradients, so thermal control to reduce gradients required attention.

## 3. FINAL DESIGN

### 3.1. Thermal Considerations

By considering thermal performance during the lens design phase, a lens form was selected that minimized focus change

**Lens A**

Focal Length = 59.3 mm

Field of View = ±14.9°

Overall Length = 111 mm

**Lens B**

Focal Length = 73.4 mm

Field of View = ±12.1°

Overall Length = 124 mm

**Lens C**

Focal Length = 95.3 mm

Field of View = ±9.4°

Overall Length = 144 mm

**Lens D**

Focal Length = 123.8 mm

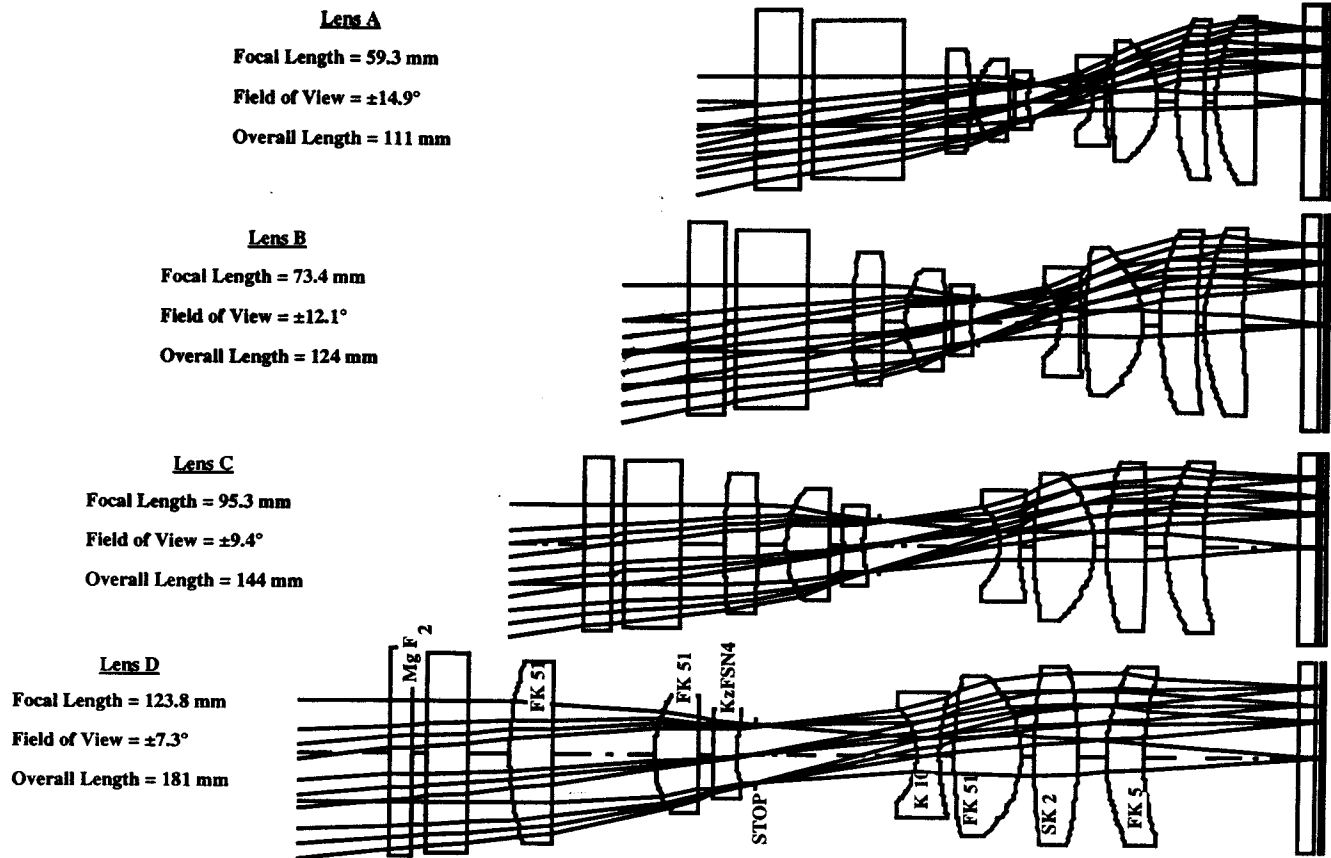Field of View = ±7.3°

Overall Length = 181 mm

Figure 4. The Four MISR Lens Designs

during thermal excursions. Even so, thermal focus compensation was required. Thermal analysis of the lens design indicated two important facets of the compensation: that the most efficient location to compensate was the space between the last lens element and the detector; and that the perfect housing material for the lens would have a higher thermal coefficient of expansion than aluminum to maintain focus. As a result, aluminum was chosen for the lens housing material and a thermal compensation assembly was designed that would move the detector into focus with temperature.

The thermal compensation assembly for the detector consisted of a set of stacked tubes of different materials as shown in Figure 5. Thermal conductivity was important in the design. The detector was cooled with a thermal electric cooler to -10°C and were insulated from surrounding structures. This was accomplished by coating the detector housing with a layer of gold to reduce emissivity, mounting the cold structures to a thin fiberglass tube (with low thermal conductivity), and by wall papering the fiberglass tube with low-emissivity aluminized mylar. The other tubes in the assembly were metallic with high thermal conductivity. They were all bonded to aluminum fittings. The thermal gradients resulting were analyzed and included in the design of the system. Since modularity was desired, the design was optimized for the mid-focal length lens – lens B. Thus lenses A, C, and D weren't perfectly focused with temperature, but they did perform within specifications within a limited temperature range. The thermal analysis of the instrument indicated that the temperature could be controlled to within this range, so this became the driving requirement for the operational temperature range for the lenses. Since the compensation assembly was designed for lens B, this lens can operate within specifications over a much larger thermal range. The other three lenses drift out of focus when the temperature range gets larger. This compromise gave the design the cost-saving advantage of using only one design for all nine cameras.

## 3.2 Other Thermal Considerations

Thermal gradients between the camera head and the lens would cause the focus compensation assembly in the camera head to compensate for a different temperature than the lens experiences. Complicating the situation further, the lens and camera head were shimmed together and shims are not a good thermal path. Additionally, the power dissipated from the Thermal

ALUMINUM  MAGNESIUM  ALUMINUM

INVAR

ALUMINUM

DETECTOR

TITANIUM

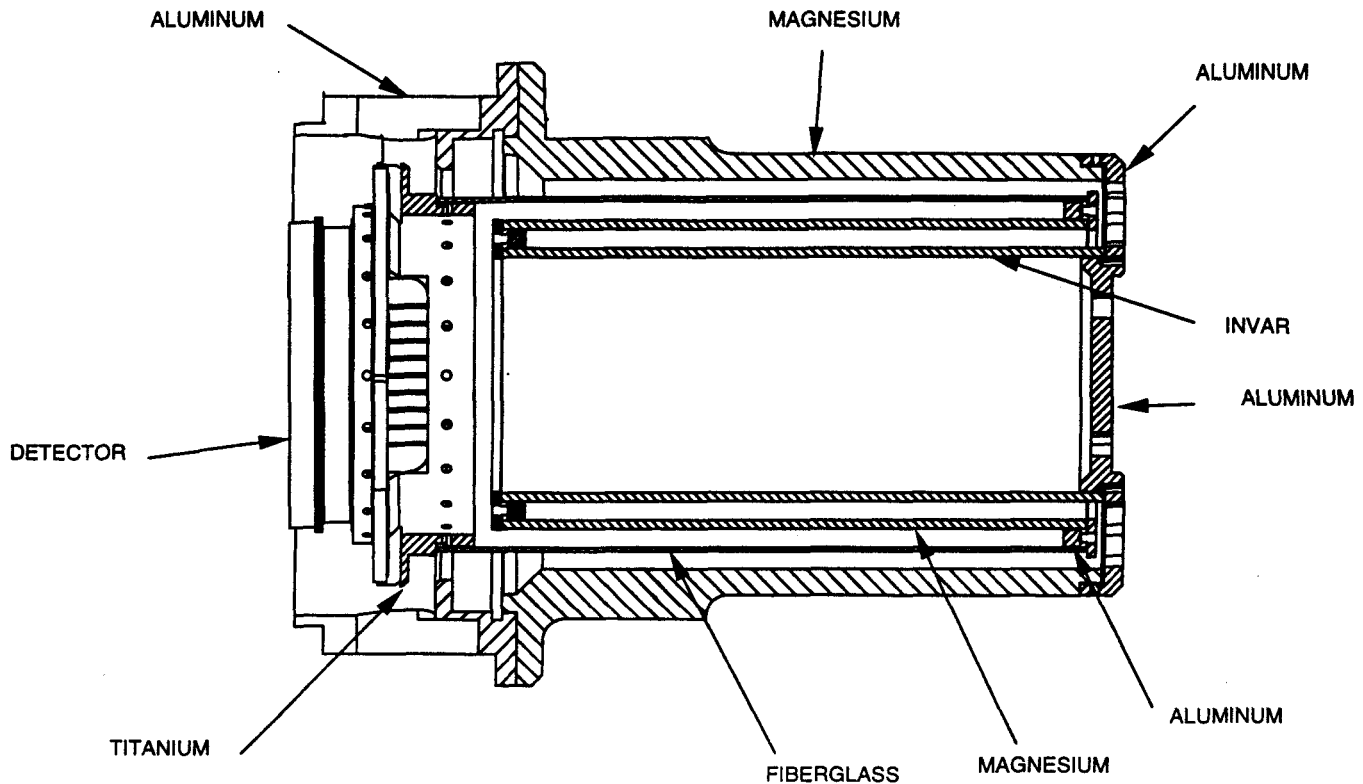FIBERGLASS  MAGNESIUM  ALUMINUM

Figure 5. Passive Thermal Focus Compensation Assembly

Electric Cooler (TEC) used to cool the detector and from the pre-amp of the detector had to be carried away. The pre-amp housing is connected to the outside of the camera head housing. Figure 2, the Camera D Assembly, shows the thermal control hardware designed to minimize temperature difference between the camera head and the lens and to carry the heat from the TEC and the electronics to the optical bench. It consists of parts made of Aluminum Alloy 7073 which has very high coefficient of thermal conduction. The parts clamp on to a conductive finger that carries heat from the TEC and the pre- amp. One end screws into the outer housing of the thermal focus compensation assembly. The other end screws onto the flange at the end of the lens barrel. Soft, annealed, pure aluminum shims were squeezed between the parts to create an effective thermal path at the joints. The parts bridge over the shimming section of the camera and connect the focus compensation assembly to the lens barrel. The lens barrel is so thick that it carried the heat to the optical bench where it can be radiated away.

### 3.3. Lens Positioning Considerations

Research into previous lens mounting techniques at JPL indicated that square-contact positioning systems on convex lenses had not survived launch loads. Tangent-contact on convex lenses had survived launch vibration.in past systems as long as the contact pressure was not extremely high. When contact pressure was extremely high, then the lenses would fail during thermal excursions. The pressure position would slide along the lens surface as the geometry between the housing, spacers and lens changed due to different coefficients of thermal expansion (CTE) of the materials involved. When the contact pressure is very high, friction is generated that can cause chipping of the lens surface when the parts slide during thermal excursions. The first configuration investigated for the MISR lenses was one with the lenses and spacers stacked with a spring all retained by a retaining ring. When the mass of the lenses and spacers was calculated and the spring was sized to

hold the components firmly during launch, the resulting force was large enough to cause the lens chipping phenomenon. This concept was not pursued.

Centering methods for lenses in housings depends on the centering tolerance required by the lens design, the size of the lenses and the difference in CTE between the housing and the lenses. For the MISR lenses, the material chosen for the housing was aluminum to accommodate the thermal focus requirements of the lens and for ease of machining. A table was generated to compare the diametral expansion and contraction of each lens to the housing to see if centering could be achieved directly from the inner diameter of the housing. Since aluminum has a high CTE and most lens materials have low CTEs, it was no surprise that clearances that prevented over-compression of the lenses throughout the survival temperature range were too large to hold the lenses within tolerances in the operational temperature range required. Since the tangent-contact spacers also can center convex lenses, that technique was chosen for MISR.

Figure 6 shows the largest lens, Lens D, and illustrates the final concept for the lens housings for MISR. Each convex lens element is held in place with tangent-contact spacers. The tangent-contact spacers hold the convex lens axially and center it. The outer diameter of one spacer for each lens is a close-fit with the inner diameter of the housing to provide the centering register. The tangent-contact spacers were made of aluminum to maximize the possibility to successfully machine the correct angle and thickness and to match the CTE of the housing. Each retaining ring clamps several lenses and spacers to save costs – threading the lens housing is expensive and can cause machining errors that result in rejection of the housing. The retaining rings were also made of aluminum with a thin clear anodize coating.

To control the clamping force under each retaining ring, spacers made of Vespel SP1 are included in each clamped stack-up of parts. The thickness of the Vespel SP1 spacers is calculated to compensate for the difference in CTE between the housing, the spacers and the lenses. Vespel SP1 has a higher CTE than aluminum. If the equation:

$$CTE_{vespel} * TH_{vespel} + CTE_{lens} * TH_{lens} + CTE_{spacer} * TH_{spacer} = CTE_{housing} * TH_{housing} \tag{1}$$

is satisfied, the force of the retaining ring holding the lenses will remain constant during thermal excursions. The retaining rings were installed with a torque of 5 inch-ounces. This provided a light force to hold the parts firmly during launch and was also enough to accommodate errors in the balance of equation (1) due to variation in the CTE values of the materials involved.
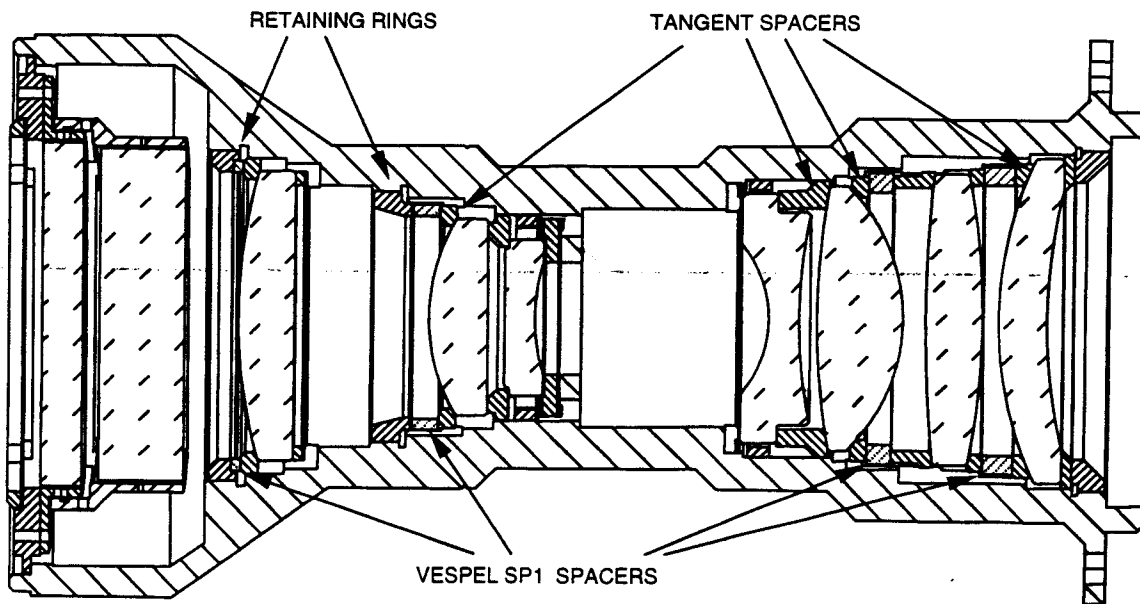


Figure 6. Section View of Lens D

A different method was developed for centering concave lenses. Figure 7 shows a typical centering ring developed to center the concave lenses in MISR. The material used was Vespel SP1 because it is clean, stable dimensionally, easy to machine,

and has been used for flexible components in the past. The parts were made first in a lathe set-up to machine tight-toleranced inner and outer diameters, then the flexure features were machined in a fixture on a mill using computer-controlled machining. The centering ring fits within the housing with a close sliding fit, and the lens fits within the centering ring with a close sliding fit.
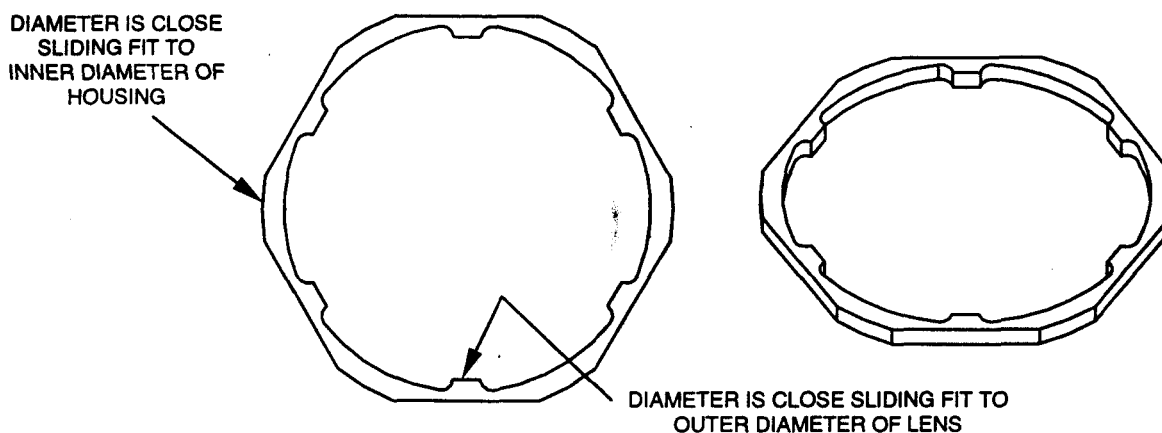
DIAMETER IS CLOSE
SLIDING FIT TO
INNER DIAMETER OF
HOUSING

DIAMETER IS CLOSE SLIDING FIT TO
OUTER DIAMETER OF LENS

Figure 7. Vespel SP1 Centering Ring for Concave Lens Elements

## 4. ASSEMBLY

The detectors and the lenses were assembled in separate laboratories by different technicians. Cleanliness was maintained in both areas. In theory, the lens parts were stacked into the housings, the retaining rings were torqued, a small vibration table was used to seat the parts, and then the retaining rings were retorqued. The performance was monitored between the assembly of each retaining ring group of lenses. In practice, it was hard to center some of the convex lenses so additional centering rings were manufactured to pre-center these lenses. These rings were simple rectangular cross-section aluminum rings. They did not constrain the lenses to within the centering tolerance limit, but were tighter fit around the lenses than the housing. They constrained the lenses from being shifted off-center too much. We believe the problem occurred because we weren't careful about the finish on the angled surface of the tangent-contact spacers. During the brass-board stage we had manufactured parts and some had fine finish call outs and some did not. All the finishes were very fine - we saw no difference in performance. When the flight parts were machined, the finish call outs were considered unnecessary because of other tight tolerances and our success with the brass board parts. The finish on these surfaces was not as fine as for the brass-board hardware and too much friction was generated that prevented the lenses from sliding into a centered position. Fine finish call outs are recommended.

## 5. TESTING

The lens was assembled with a detector housing then tested to determine the shimming required for tilt and focus adjustment. Detailed descriptions of the measurements and the measuring equipment are in the following papers:

E. Hochberg, M. White, R. Korechoff, C. Sepulveda, "Optical Testing of MISR lenses & cameras", in SPIE's International Symposium on Optical Science, Engineering, & Instrumentation in Denver, Colorado, 4-9 August 1996, Earth Observing System Conf. Proc. Vol. 2830, pp. 286-293.

E. Hochberg, N. Chrien "Lloyd's mirror for MTF testing of MISR CCD", in SPIE's International Symposium on Optical Science, Engineering, & Instrumentation in Denver, Colorado, 4-9 August 1996, Earth Observing System Conf. Proc. Vol. 2830, pp. 274-285.

To summarize the process briefly, the optimum focal plane for a lens was determined with the use of a collimator/target projector which presented a point source at infinity to the lens under test (LUT). Microscopic examination of the aerial image of this point source formed by the LUT at various field positions and through various focal planes was the basis for the determination of the optimum focal plane. The two-dimensional focal plane "spots" were Fourier-transformed to produce an

MTF value at the detector Nyquist spatial frequency (23.8 c/mm) for that field point and focal plane position. An ensemble of 840 discrete MTF measurements over the field and through-focus were considered when determining the optimum focal plane. Automated measurements were made with respect to wavelength, temperature, field of view, orientation (horizontal or vertical) and spatial frequency. All of these MTF measurements were spatially referenced to a mechanical feature on the lens/camera interface flange. Information describing the explicit location (piston & tilt) of this optimum focal plane was used to precisely locate the CCD detector array relative to the back flange of the lens - the optimization criteria was to maximize the lowest MTF seen anywhere in the field. Shims were calculated to place between the two assemblies to place the detector array at the derived location.

The shimming was done at an intermediate flange between the lens assembly and the camera head assembly. Three pads were provided to enable tilt and axial position adjustment. The interfacing surface of the flange was toroidal in shape to accommodate tilting. Figure 8 shows the shimming pad locations.

# 6. RESULTS

## 6.1. Dynamic Testing

After assembling and shimming, each camera was tested to launch-level vibration loads. The performance of the lenses was measured after the vibration testing to determine changes. The MTF of all lenses improved slightly after the vibration testing.
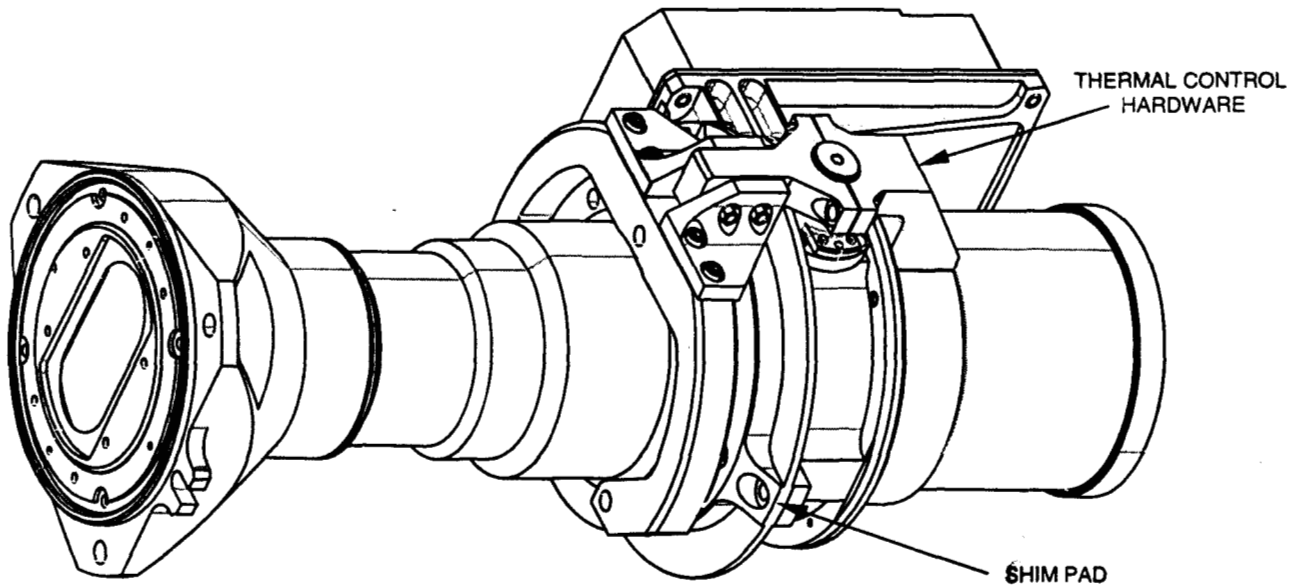


Figure 8. Assembled Camera D

## 6.2. Thermal Testing

The performance of the cameras was measured during the thermal cycle testing through the operational temperature range. Since the focus compensation was tuned to the B lens, the other lenses were expected to lose focus when the temperature varied from 5°C. The lenses performed just as predicted. The B camera maintained focus throughout the thermal range. The other lenses defocused slightly, but remained within tolerances. All the lenses survived the thermal cycling through the survival temperature range. Performance was measured after the survival temperature cycling was completed. No performance change was detected.

# 7. ACKNOWLEDGEMENTS